Research on Manipulation Strategy of Quad Tilt-Rotor

WANG Zhigang[1*], *LYU Zhichao*[1], *LI Jianbo*[2]

1. Yangzhou Collaborative Innovation Research Institute, Shenyang Aircraft Design & Research Institute, Yangzhou 225000, P. R. China;

2. National Key Laboratory of Science and Technology on Rotorcraft Aerodynamic, College of Aerospace Engineering, Nanjing University of Aeronautics and Astronautics, Nanjing 210016, P. R. China

(Received 29 July 2020; revised 10 October 2020; accepted 13 October 2020)

Abstract: Aiming at the complex tilting process of quad tilt-rotor (QTR) transition mode, this paper studies the manipulation strategy in transition mode to solve the problem of manipulation redundancy and coupling in transition mode of quad tilt rotor. The variations of the manipulation derivative are analyzed in the tilting process. Through the flight control simulation and flight test of the quad tilt-rotor, the validity of the control system and the rationality of the manipulation strategy are verified.

Key words: quad tilt-rotor; manipulation strategy; flight test; simulation

CLC number: V19 **Document code:** A **Article ID:** 1005-1120(2020)S-0001-08

0 Introduction

The quad tilt-rotor[1] (QTR) is a novel vehicle which combines the characteristics of helicopters and planes. QTR has three flight modes: the helicopter mode, plane mode and the transition mode. QTR has two sets of helicopter and plane manipulation modes, and gradually transforms with the change of the nacelle tilt angle[2]. Therefore, the manipulation redundancy of QTR will appear in the transition process. In addition, the whole tilting transition process must be completed within the transition corridor. How to solve the problem of manipulation redundancy and make QTR successfully complete the conversion between the helicopter and the plane mode is an important research topic[3-6].

At present, the control methods of QTR in the transition mode focus on the preset control scheme to solve the problem of manipulation redundancy, and the control system is designed to track the predetermined commands[7-10] (tilting law, flight trajectory, etc.). It is impossible to obtain the optimal manipulation strategy and flight trajectory of the whole tilting process under different flight missions[11-13]. In fact, studying the optimal transition process will obtain the corresponding manipulation strategy. This can not only solve the problem of manipulation redundancy, but also effectively improve the tilting efficiency. Therefore, it is necessary to study the optimal tilt path of QTR.

1 Aerodynamic Model

The quad tilt rotor with partial tilt wings in this paper is shown in Fig.1. It includes four groups of

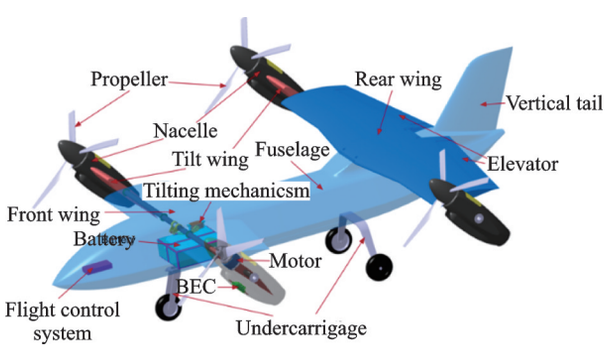

Fig.1 Quad tilt-rotor with partial tilt wing

*Corresponding author, E-mail address: wangzhigang@nuaa.edu.cn.

How to cite this article: WANG Zhigang, LYU Zhichao, LI Jianbo. Research on manipulation strategy of quad tilt-rotor[J]. Transactions of Nanjing University of Aeronautics and Astronautics, 2020, 37(S): 1-8.

http://dx.doi.org/10.16356/j.1005-1120.2020.S.001

propellers, front and rear wings, a fuselage, an elevator, motors, the tilting mechanism, an undercarriage and the flight control system.

The parameters[14] of the quad tilt rotor with partial tilt wings are shown in Table 1.

Table 1 Parameters of quad tilt rotor

Category	Item	Value	
Propeller	Radius/inch	20	
	Blade number	2	
	Thread pitch/inch	*m*	
Wing parameter		Front	Rear
	Wing area/m^2	0.28	0.475
	Tilt wing area/m^2	0.042 5(One side)	
	Wingspan/m	1.3	1.8
	Taper ratio	1.2	1.5
	Mean-chord/m	0.265	0.3
	Aspect ratio	4.9	6
	Airfoil profile	Eppler1200	
Fuselage parameter	Length/m	1.8	
	Maximum cross-sectional area/m^2	0.06	
Relative position parameter	Vertical distance of front and rear wings/m	0.08	
	Vertical distance of the two propellers on the same side/m	0.08	
	Horizontal distance of the two propellers on the same side/m	0.26	

Nonlinear dynamic model of the quad tilt-rotor can be described as

$$\dot{\boldsymbol{X}} = f(\boldsymbol{X}, \boldsymbol{U}, t) \tag{1}$$

where X is the system state variable, $\boldsymbol{X} = [u\ v\ w\ p\ q\ r\ \varphi\ \vartheta\ \psi]$; $\boldsymbol{U}$ the system control variable, which includes the throttle manipulation δ_T, the longitudinal manipulation δ_E, the lateral manipulation δ_A, the course manipulation δ_R and the tilt angle β_m.

$$\boldsymbol{U} = [\ \delta_T \quad \delta_E \quad \delta_A \quad \delta_R \quad \beta_m\ ] \tag{2}$$

The Taylor series expansion of Eq.(2) is carried out at the equilibrium point. Keeping the linear part and ignoring the higher order part, we can get

$$\Delta\dot{\boldsymbol{X}} = \frac{\partial f}{\partial \boldsymbol{X}}\Big|_{\boldsymbol{X}_{\text{trim}}} \Delta\boldsymbol{X} + \frac{\partial f}{\partial \boldsymbol{U}}\Big|_{\boldsymbol{U}_{\text{trim}}} \Delta\boldsymbol{U} \tag{3}$$

where the subscript *trim* indicates the trimming value, $\Delta\boldsymbol{X}$ and $\Delta\boldsymbol{U}$ are the increments of system state variables and system control variables, respectively. Eq.(3) can be rewritten as

$$\Delta\dot{\boldsymbol{X}} = \boldsymbol{A}\Delta\boldsymbol{X} + \boldsymbol{B}\Delta\boldsymbol{X} \tag{4}$$

where $\boldsymbol{A}$ is the system state matrix, which is composed of partial derivatives of forces and moments with respect to state variables; $\boldsymbol{B}$ the control matrix, which is composed of partial derivatives of forces and moments with respect to control variables, namely, the manipulation derivative matrix. It also reflects the aerodynamic change generated by the unit control quantity, which reflects the control efficiency of the control input to the vehicle.

$$\boldsymbol{B} = \begin{bmatrix} \partial F_x/\partial\delta_T & \partial F_x/\partial\delta_E & \partial F_x/\partial\delta_A & \partial F_x/\partial\delta_R & \partial F_x/\partial\beta_m \\ \partial F_y/\partial\delta_T & \partial F_y/\partial\delta_E & \partial F_y/\partial\delta_A & \partial F_y/\partial\delta_R & \partial F_y/\partial\beta_m \\ \partial F_z/\partial\delta_T & \partial F_z/\partial\delta_E & \partial F_z/\partial\delta_A & \partial F_z/\partial\delta_R & \partial F_z/\partial\beta_m \\ \partial M_x/\partial\delta_T & \partial M_x/\partial\delta_E & \partial M_x/\partial\delta_A & \partial M_x/\partial\delta_R & \partial M_x/\partial\beta_m \\ \partial M_y/\partial\delta_T & \partial M_y/\partial\delta_E & \partial M_y/\partial\delta_A & \partial M_y/\partial\delta_R & \partial M_y/\partial\beta_m \\ \partial M_z/\partial\delta_T & \partial M_z/\partial\delta_E & \partial M_z/\partial\delta_A & \partial M_z/\partial\delta_R & \partial M_z/\partial\beta_m \\ 0 & 0 & 0 & 0 & 0 \\ 0 & 0 & 0 & 0 & 0 \\ 0 & 0 & 0 & 0 & 0 \end{bmatrix} \tag{5}$$

2 Tilt Angle of Nacelle

The maximum and minimum velocities under each tilt angle are calculated, and then the transition corridor of QTR with tilt wing are obtained. The boundary of a small velocity is mainly determined by whether the wing reaches the stall angle of attack, and the maximum velocity boundary is mainly determined by whether the propeller power reaches the maximum power.

Fig.2 shows the calculated tilt transition corridor. The tilt angle is 90° for the helicopter mode; and 0° for the plane mode. The black line is the boundary of the minimum velocity of QTR with tilt wings. And the red line is the boundary of the maximum speed of QTR with tilt wings.

The vehicle transition switching is a variable velocity and structure process which must reasonably control the aerodynamic distribution between the propellers and the wings. If the forward velocity is too small, it will lead to the stalled wing. Therefore, the transition mode is a process of controling the altitude, the forward velocity and the tilt angle. The change of tilt angle β_m of the nacelle is as follows

$$\beta_m = \omega_\beta \cdot t \tag{6}$$

where ω_β is the tilt velocity based on altitude and forward velocity and t the tilt time.

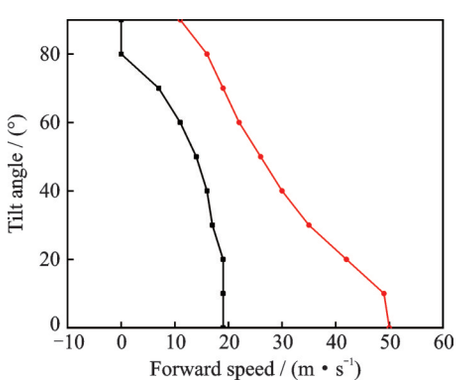

Fig.2 Tilt transition corridor

3 Manipulation Distribution

Fig.3 shows the curves of manipulation derivatives with forward velocity in the transition mode.

It can be seen from Figs.3 (a), (b) and (c) that with the increase of the forward velocity, the manipulation efficiency of δ_T, δ_E and δ_A are enhanced. As observed, the two manipulation deriva-

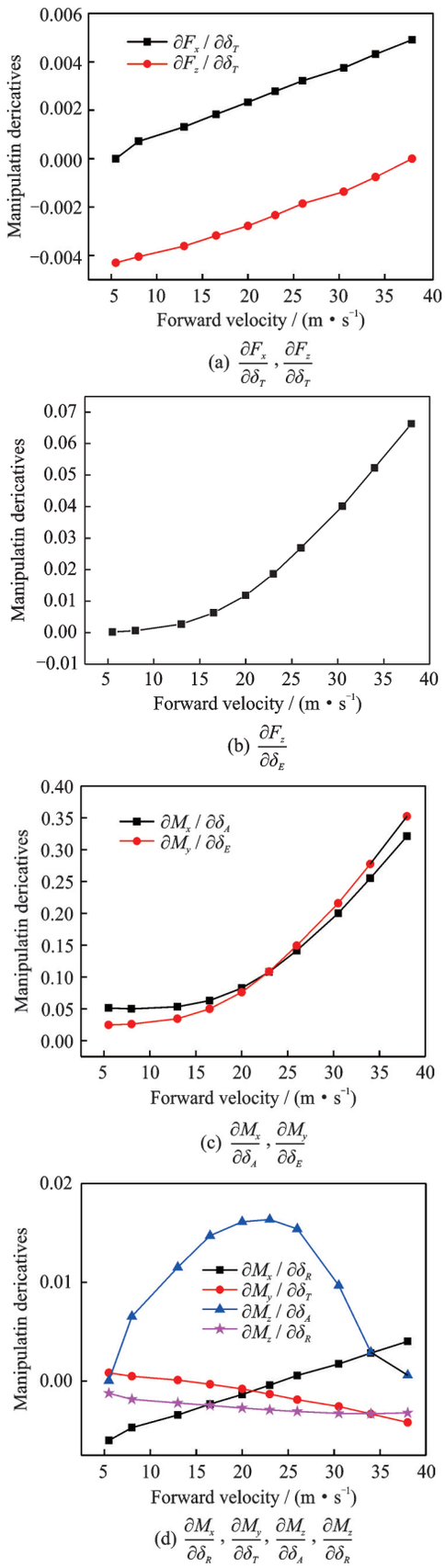

Fig.3 Curves of manipulation derivatives

tives of $\partial F_x/\partial\delta_T$ and $\partial F_z/\partial\delta_T$ are essentially linear. However, the manipulation derivatives of $\partial F_z/\partial\delta_E$, $\partial M_x/\partial\delta_A$ and $\partial M_y/\partial\delta_E$ have obvious non-monotonicity. For vertical position control, δ_T and δ_E are redundant. With the increase of β_m, the manipulation efficiency of δ_T decreases and the manipulation efficiency of δ_E increases. From Fig.3(d), we can know that with the increase of the forward velocity, the manipulation derivative of $\partial M_x/\partial\delta_R$ increases, but the manipulation derivatives of $\partial M_y/\partial\delta_T$ and $\partial M_z/\partial\delta_R$ decreases. The manipulation derivative of $\partial M_z/\partial\delta_A$ increases and then decrease with the increases of the forward velocity. From Figs.3(c), (d), we can see that in the transition mode, δ_T and δ_E have redundant manipulations for pitch. The manipulation efficiency of δ_E is enhanced with the increase of the forward speed while the manipulation efficiency of δ_T is receded. The lateral and course have coupling manipulations. The effect of δ_A on the course coupling is greater than that of δ_R on the lateral coupling. Especially, the manipulation efficiency of δ_A on course is enhanced with the tilt angel β_m increaing at the beginning. However, when the tilt angle reaches a certain value, the manipulation efficiency of δ_A on course is receded. Therefore we can know from Fig.3 the forward velocity and tilt angle β_m have great influence on the manipulation derivatives.

In the transition mode, QTR always maintains the attitude angle and height stability to achieve a smooth transition flight. In terms of height manipulation, it is necessary to automatically compensate the propeller rotational speed and the rudder deflection angle to achieve height stability.

The height control and steering authority distribution strategy used by QTR is shown in Fig.4.

k_1, k_2, k_3, k_4 are distribution coefficient related to the tilt angle β_m and forward velocity.

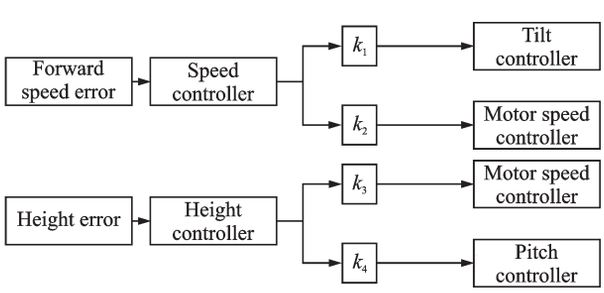

Fig.4 Manipulation distribution in transition mode

$$k_1 = ((\cos(2(\pi/2-\beta_m)))+1)/2 \tag{7}$$

$$k_2 = ((\sin(2(\pi/2-\beta_m)-\pi/2))+1)/2 \tag{8}$$

$$k_3 = \begin{cases} 1 & u<18 \\ 1-\dfrac{u-18}{20} & 18\leqslant u<38 \\ 0 & u\geqslant 38 \end{cases} \tag{9}$$

$$k_4 = \begin{cases} 0 & u<18 \\ \dfrac{u-18}{20} & 18\leqslant u<38 \\ 1 & u\geqslant 38 \end{cases} \tag{10}$$

Fig.4 shows the manipulation right distribution is required during the transition process due to the change of height and speed. The angle of the nacelle is small and the forward flying speed is low. By adjusting the speed of the propeller to change the lift of the rotor, the height can be more effectively controlled stably. In the early stage, when the speed is not established, it is necessary to change the attitude of the quad tilt rotor, while increase the rotational speed of the propeller to achieve the acceleration of the quad tilt rotor

After the quad tilt rotor retreats from the copter mode, it accelerates forward. At this time, the flight mode is switched. The simulation results are shown in Figs.5—6, where the shaded part represent the transition mode. Fig.5 shows the change of the pitch angle, the height, the forward speed and the tilt angle of the nacelle during the mode transition. It can be seen that the pitch angle of the quad tilt rotor is finally maintained at the initially set angle of 5°, and the height maintaining effect is better. The height difference is finally stabilized at about 0 m, and the forward flying speed is increased more rapidly in the transition mode. The nacelle waits for a short period of time at the set angle, and the time of the entire tilt process is about 7.5 s.

Manipulation distribution strategy is designed

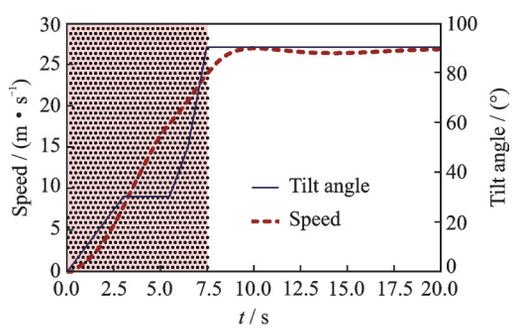

(a) Speed

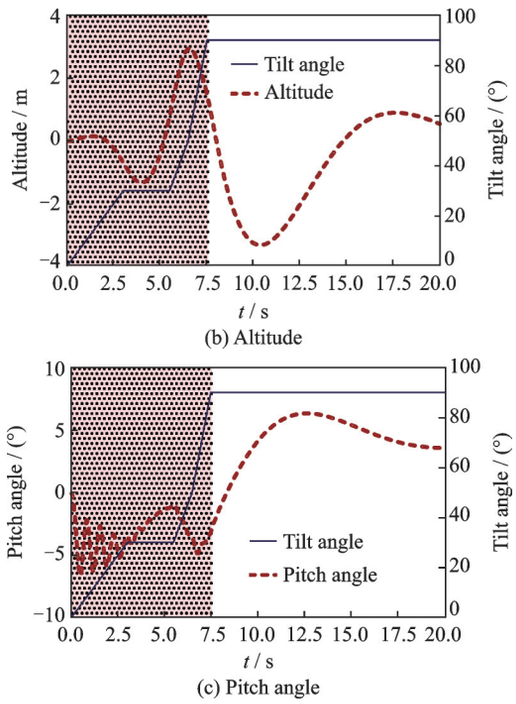

Fig.5 Changes in each channel during tilting process

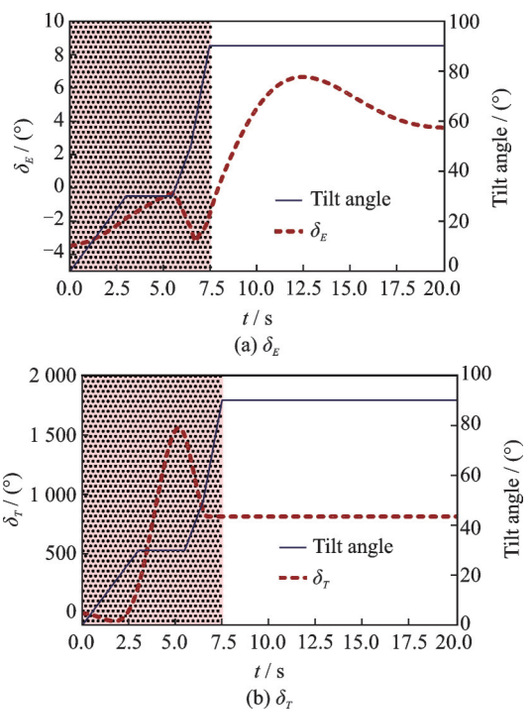

Fig.6 Manipulation compensation during tilting process

according to Fig.4. Tilting strategy is designed according to Figs.5—6. In order to compare the tilt path optimization strategy, we design other three tilting strategies.

Condition 1 Tilting with different tilt rates, and waiting for the forward speed to reach the set speed at the set tilt angle (the optimal tilt path in Figs.5—6).

Condition 2 Directly tilting from the copter mode to the plane mode at different tilt rates.

Condition 3 Tilting with one tilt rate, and waiting for the forward speed to reach the set speed at the set tilt angle.

Condition 4 Directly tilting from the copter mode to the plane mode at one tilt rate.

The tilt parameters of the four conditions are shown in Table 2.

Table 2 Parameters of four conditions

Parameters	C1	C2	C3	C4
Tilt rate 1/((°)•s^{-1})	10	10	10	10
Tilt rate 2/((°)•s^{-1})	20	20	10	10
Tilt rate 3/((°)•s^{-1})	40	40	10	10
Set speed 1/(m•s^{-1})	17.9		19.9	
Set speed 2/(m•s^{-1})	20		20	
Set tilt angle 1/(°)	30		30	
Set tilt angle 2/(°)	50		50	

Fig.7 shows the results of the flight simulation. The shaded parts represent the tilting process in the four conditions. From Fig.7 we can see that at the beginning of tilting, the forward speeds are same in all four conditions. But as the tilt angle increases, the increment of forward speed changes gradually. When the tilting process is finished, the forward speed of the four conditions are 24, 20, 22 and 30 m/s. At the beginning, the altitudes are same in all four conditions, and then the altitudes of Conditions 1, 3 and 4 increase but the altitude of condition 2 continues to decrease. The minimum altitudes of the four conditions in the tilting process are −1.3, −3.1, −5.5 and −1.6 m. When QTR turns to the plane mode, the altitudes of the four conditions change to 1.3, −3.1, −5.5 and 0.9 m. Same as the changing of the altitude and the forward speed, the pitch angles are the same at the beginning. And the pitch angles of the four conditions are −3.0, 4.5, 0.4 and 8.3°. When the tilt angle is less than 30°, the tilt rate remains the same, so when the tilt time is 3 s, the nacelle tilt angles are all 30° in the four conditions. When the tilt angle is above 30°, the nacelles continue tilting. However, the tilt angles of Conditions 2 and 4 are unchanged because of the for-

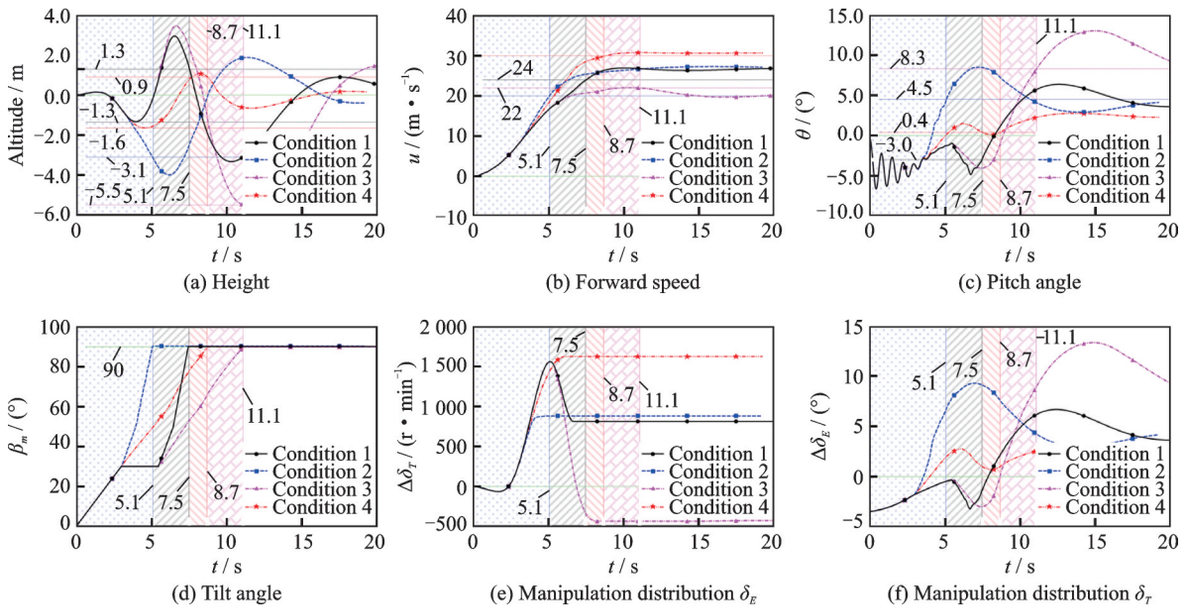

Fig.7 Curves of flight simulation results

ward speed. And it waits about 2.4 s for the forward speed reaching the set speed at tile angle 30°. In these four conditions, the time spent in the tilting process is about 5.1, 7.5, 8.7 and 11.1 s.

We can see from the results of the flight simulation (Fig.7) that in the first stage of the tilting process ($\beta_m < 30°$), the constraint conditions of the four conditions are same, so are the results. The forward speed is established slowly, hence, QTR lowers its head to speed up the forward speed according to the manipulation strategy. And then, it leads to a reduction in height. When $30° \leqslant \beta_m < 50°$, for Condition 2 and Condition 4, the nacelle continues tilting, while the nacelle of Condition 1 and Condition 3 wait for the forward speed to establish at $\beta_m = 30°$. Due to the tilt rate of Condition 2 is much faster than Condition 4, the forward speed in Condition 2 is increasing faster than the speed in condition 4 and the vertical pull in condition 2 provided by the propellers is sharply reduced. The wing's increased lift is not enough to balance the propeller's reduced vertical pull, so the height is reduced sharply which will lead the pitch angle in Condition 2 bigger than that in Condition 4 to reduce the change of height according to the manipulation strategy in Section 3. When the forward speed reaches the set speed at $\beta_m = 30°$, the results of the flight simulation in Condition 1 and Condition 3 are same to the results in Conditions 2 and 4. In the tilting process, the change of the altitude is crucial to the safety of the transition flight. The increase in altitude can be regarded as a safe state of the flight. All of the four flight conditions, we can see that the minimum altitudes of the four flight conditions are −1.3, −3.1, −5.5 and −1.6 m. Condition 1 is our most desired flight condition. And its transition time is shorter (7.5 s). Therefore, the optimization solution obtained in this paper is close to the simulation results. The pitch angle changes more smoothly, and the whole tilting process is much faster and more stable.

To verify the effectiveness of the manipulation strategy and the flight control law, the flight test are carried out. The flight results are shown in Figs.8—13.

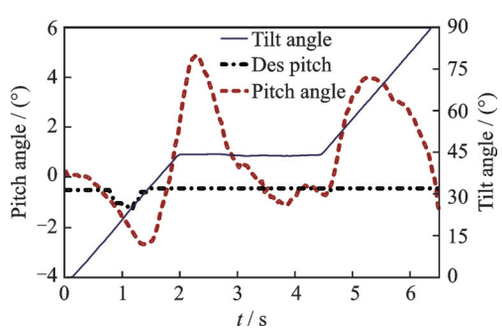

Fig.8 Pitch angle during forward tilting

As can be seen from Fig.8, the input pitch angle remains basically unchanged after the transformation. Due to the altitude control during the transition, the aircraft will adjust the pitch angle of the fuselage to maintain a stable altitude. After current flight speed reaches the minimum forward flight

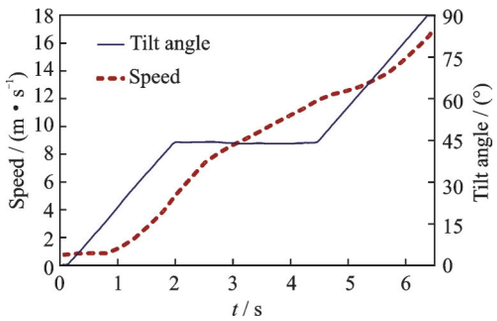

Fig.9 Speed during forward tilting

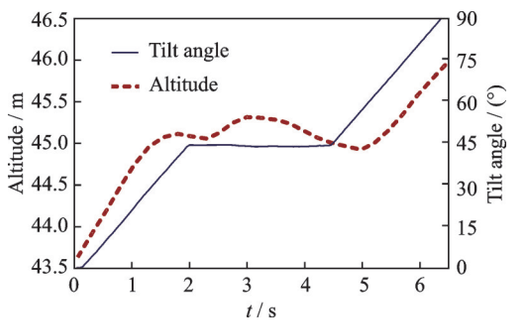

Fig.10 Altitude during forward tilting

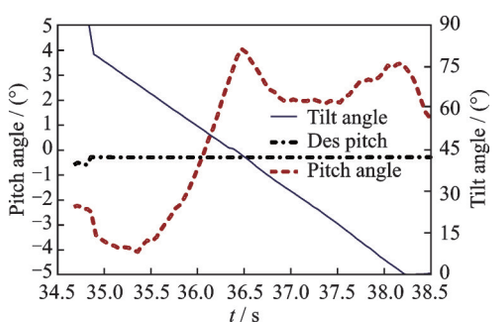

Fig.11 Pitch angle during backward tilting

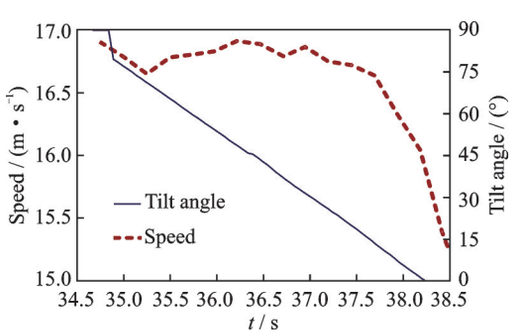

Fig.12 Speed during backward tilting

speed of the plane, the nacelle will quickly tilt to the horizontal position to complete the model transformation.

Fig.9 shows the variation of speed during the forward flight transition. At the beginning of the tilting, the forward flight speed increases more slowly. When the tilt angle is 45°, the nacelle stays at the

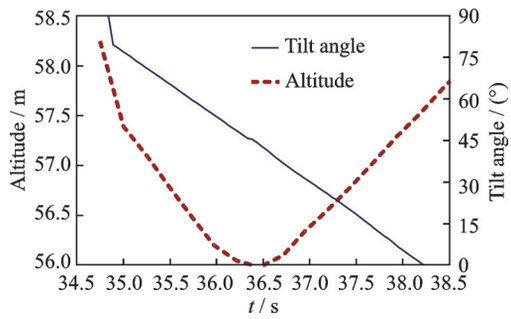

Fig.13 Altitude during backward tilting

current angle and waits for the forward speed to reach the set value (12 m/s).

Fig.10 shows the change in altitude during the entire flight. After the quad tilt rotor starts in quad mode, it begins to climb. When the height reaches 43 m, the mode transformation is carried out. During the transition, the height basically remains unchanged. After the current flying speed reaches the minimum forward flying speed of the plane, the nacelle will quickly tilt to the plane position to complete the mode conversion. The forward flying speed has already exceeded the minimum forward flying speed of the plane. At this time, the lift force provided by the wing is be greater than the gravity of the fuselage, so the altitude of unmanned aerial vehicle will increase.

Figs.11—13 are the landing transition mode. When the plane mode changes to the multi-rotor mode, the nacelle is tilting all the way up to the vertical position. At the beginning of the landing transition mode, the pitch angle is negative which will lead the altitude to decrease, and with the tilting goes on, the pitch angle increases to positive, so the altitude increases. In the whole landing transition mode, the forward speed decreases about 2 m/s.

4 Conclusions

Aiming at controling surface redundancy and channel coupling in the transition mode, the manipulation strategy is designed. The simulation and flight results show that the manipulation strategy has high control precision. The effectiveness of the control system and the rationality of the manipulation strategy have been verified.

References

[1] FLORES G R, ESCAREÑO J, LOZANO R, et al. Quad-tilting rotor convertible MAV: Modeling and real-time hover flight control[J]. Journal of Intelligent & Robotic Systems, 2012,65(1/2/3/4): 457-471.

[2] PAPACHRISTOS C, ALEXIS K, TZES A B T C. Hybrid model predictive flight mode conversion control of unmanned quad-tilt rotors[C]//Proceedings of Control Conference (ECC), 2013 European. [S.l.]: IEEE, 2013.
[3] KIM C J, SUNG S, PARK S H, et al. Numerical time-scale separation for rotorcraft nonlinear optimal control analyses[J]. Journal of Guidance Control & Dynamics, 2014,37(2): 658-673.
[4] BOTTASSO C L, CROCE A, LEONELLO D, et al. Optimization of critical trajectories for rotorcraft vehicles[J]. Journal of the American Helicopter Society, 2005,50(2): 165-177.
[5] CHAO D, BAI H, ZENG J B T G. Nonlinear stabilization control of tilt rotor UAV during transition flight based on HOSVD[C]//Proceedings of Guidance, Navigation & Control Conference. [S. l.]: IEEE, 2017.
[6] PU Huangzhong, ZHEN Z, GAO C. Tiltrotor aircraft attitude control in conversion mode based on optimal preview control[C]//Proceedings of China Academic Conference on Guidance, Navigation and Control.[S.l.]: [s.n.], 2014.
[7] CARLSON E B, ZHAO Y J. Prediction of tiltrotor height velocity diagrams using optimal control theory[J]. Journal of Aircraft, 2015,40(5): 896-905.
[8] OKUNO Y, KAWACHI K. Optimal takeoff procedures for a transport category tiltrotor[J]. Journal of Aircraft, 2014,30(30): 291-292.
[9] COLUNGA G R F, LOZANO R B T I. Transition flight control of the quad-tilting rotor convertible MAV[C]//Proceedings of 2013 International Conference on Unmanned Aircraft Systems (ICUAS).[S. l.]: IEEE, 2013.
[10] FLORES-COLUNGA G R, LOZANO-LEAL R. A nonlinear control law for hover to level flight for the quad tilt-rotor UAV[J]. IFAC Proceedings Volumes, 2014,47(3): 11055-11059.
[11] OOSEDO A, ABIKO S, NARASAKI S, et al. Large attitude change flight of a quad tilt rotor unmanned aerial vehicle[J]. Advanced Robotics, 2016, 30(5): 326-337.
[12] LI Haixu, QU Xiangju. Multi-body motion modeling and simulation for tilt rotor aircraft[J]. Chinese Journal of Aeronautics, 2010,23(4): 415-422.
[13] XIA Q Y, XU Jinfa, ZHANG L, et al. Redundant manipulation control strategy for unmanned tilt-rotor aircraft[J]. Journal of Harbin Institute of Technology, 2014, 46(1): 121-128.
[14] WANG Zhigang, ZHAO Hong, DUAN Dengyan, et al. Application of improved active disturbance rejection control algorithm in tilt quad rotor[J]. Chinese Journal of Aeronautics, 2020, 33(6): 1625-1641.

Acknowledgement This work was supported by the Priority Academic Program Development of Jiangsu Higher Education Institutions (PAPD).

Author Dr. **WANG Zhigang** received the B.S. degree in space science and technology and the M.S. degree in software engineering from Harbin Institute of Technology, Harbin, China, in 2012 and 2014, respectively. He received the Ph.D. degree in aerospace vehicle design from Nanjing University of Aeronautics and Astronautics, Nanjing, China in 2020. Now, he works at the Yangzhou Collaborative Innovation Research Institute, Shenyang Aircraft Design & Research Institute as an engineer. His research is focused on flight dynamics and flight control design of traditional and tandem helicopter and tilt-rotor aircraft.

Author contributions Dr. **WANG Zhigang** and Prof. **LI Jianbo** designed the study. Dr. **WANG Zhigang** complied the models, conducted the analysis, and interpreted the results. Dr. **WANG Zhigang** and Ms. **LYU Zhichao** wrote the manuscript. Dr. **WANG Zhigang** performed the figure generation. All authors commented on the manuscript draft and approved the submission.

Competing interests The authors declare no competing interests.

(Production Editor: XIA Daojia)

倾转四旋翼操纵策略研究

王志刚[1],吕志超[1],李建波[2]

(1.沈阳飞机设计研究所扬州协同创新研究院有限公司,扬州 225000,中国;2.南京航空航天大学旋翼动力学国家级重点实验室,南京 210016,中国)

摘要:针对倾转四旋翼复杂的倾转过渡过程,研究了过渡模态下的操纵策略用来解决倾转四旋翼在过渡模式下的操纵冗余问题。在倾转过程中,分析了操纵导数的变化。并通过对倾转四旋翼的飞行控制仿真和试飞试验,验证了控制系统的有效性和操纵策略的合理性。

关键词:倾转四旋翼;操纵策略;飞行试验;仿真